



Field-tuned critical fluctuations in $\text{YFe}_2\text{Al}_{10}$: Evidence from magnetization, ^{27}Al NMR, and NQR investigations

P. Khuntia,^{1,*} A. M. Strydom,² L. S. Wu,^{3,4} M. C. Aronson,^{3,4} F. Steglich,¹ and M. Baenitz¹

¹Max Planck Institute for Chemical Physics of Solids, 01187 Dresden, Germany

²Physics Department, University of Johannesburg, P.O. Box 524, Auckland Park 2006, South Africa

³Brookhaven National Laboratory, Upton, New York 11973, USA

⁴Department of Physics and Astronomy, Stony Brook University, Stony Brook, New York 11794, USA

(Received 28 September 2012; published 6 December 2012)

We report magnetization, specific heat, and NMR investigations on $\text{YFe}_2\text{Al}_{10}$ over a wide range of temperature and magnetic field and zero field (NQR) measurements. Magnetic susceptibility, specific heat, and spin-lattice relaxation rate divided by $T(1/T_1T)$ follow a weak power law ($\sim T^{-0.4}$) temperature dependence, which is a signature of the critical fluctuations of Fe moments. The value of the Sommerfeld-Wilson ratio and the linear relation between $1/T_1T$ and χ suggest the existence of ferromagnetic correlations in this system. No magnetic ordering down to 50 mK in $C_p(T)/T$ and the unusual T and H scaling of the bulk and NMR data are associated with a magnetic instability which drives the system to quantum criticality. The magnetic properties of the system are tuned by field wherein ferromagnetic fluctuations are suppressed and a crossover from quantum critical to Fermi-liquid behavior is observed with increasing magnetic field.

DOI: [10.1103/PhysRevB.86.220401](https://doi.org/10.1103/PhysRevB.86.220401)

PACS number(s): 71.27.+a, 74.40.Kb, 76.60.-k, 71.10.Hf

Critical fluctuations (CFs) close to absolute zero in temperature in materials as diverse as heavy-fermion systems,¹⁻⁴ cuprates,^{5,6} and iron pnictides⁷ intimate the proximity to a quantum critical point (QCP). Whether or not the quantum critical point is underpinned by a magnetic phase transition depends on the location of the material on the generic phase diagram that connects a paramagnetic ground state with antiferromagnetic (AFM) order through an intervening QCP. The spatial dimensionality of the material has been demonstrated recently as an insightful ingredient in tuning the degree of fluctuations and the physics of quantum criticality.⁸ Controlling a magnetic phase transition by means of a tuning parameter such as chemical composition, magnetic field (H), or pressure has proven to be a profitable route to QC.^{4,9} Non-Fermi-liquid (NFL) behavior of thermal properties is a hallmark of QC. The T and H scaling of magnetic systems is an intrinsic metric to unravel details such as the universality of quantum phase transitions (QPTs). For instance, unusual scaling in the resistivity $\rho(T) \sim T^n$ ($n < 2$), specific heat $C_p(T)/T \sim [-\ln T \text{ or } T^{-(n)} (n < 1)]$, and magnetic susceptibility $\chi(T) \sim T^{-n}$ ($n < 1$) at low T are associated with QPT.¹⁻⁴ A QPT typically causes a pileup of entropy towards $T \rightarrow 0$. The NFL behavior in the local probe NMR leads to unusual power laws in spin-lattice relaxation rates (SLRs) with $1/T_1T \sim T^{-n}$ ($n < 2$) in the $T \rightarrow 0$ limit, in contrast to simple local moment metals wherein $n = 0$ is expected. From a theoretical point of departure, NFL behavior displaying these T scaling relations is native to instabilities in correlated electron systems, and spin fluctuations (SFs) may also display similar NFL-like divergences. The concept of QC in $4f$ - and $3d$ -electron spin-density-wave systems in which an appropriate tuning parameter dissolves AFM order into a paramagnetic FL is by now well established.^{1-4,10,11} For instance, in YbRh_2Si_2 , small fields suppress the AFM order and $1/T_1T \sim T^{-0.5}$ is observed, which is due to a delicate interplay between FM and AFM spin fluctuations of local Yb^{3+} moments in the vicinity of a QCP.^{12,13} The significance

of SFs and their field dependence in itinerant ferromagnets (FMs) such as MnSi ,¹⁴ $\text{Y}(\text{Co}_{1-x}\text{Al}_x)_2$,¹⁵ ZrZn_2 ,¹⁶ Ni_3AlC_x ,¹⁷ $\text{Sr}_{1-x}\text{Ca}_x\text{RuO}_3$,¹⁸ Sc_3In ,¹⁹ and LaCoPO (Refs. 20 and 21) have been explained by NMR in the framework of the self-consistent renormalization (SCR) theory.²² The notion of QC when the order parameter is FM, on the other hand, is controversial and currently a subject of debate. Recently, weak FM systems such as UGe_2 ,²³ MnSi ,²⁴ and ZrZn_2 ,²⁵ and NbFe_2 (Refs. 26 and 27) have been showing exciting features, and it is observed that the magnetic field and/or pressure act as tuning parameters. Furthermore, unusual and weak power laws in $\chi(T)$ and $C_p(T)/T$ due to atomic disorder in a few itinerant and local moment systems are interpreted by a quantum Griffith phase model.²⁸⁻³⁷ The scaling behavior of observables especially in T and H offer a systematic approach towards establishing universality classes. In QC systems, however, our current understanding of the energy scaling that drives cooperative behavior offers very little commonality. The QC region of phase space appears to offer increasing layers of detail which complicate a consistent treatment of the QC region among different materials. The idea of universality still appears to be a distant target of our understanding of quantum criticality.

Ternary orthorhombic $4f$ aluminides of $\text{RT}_2\text{Al}_{10}$ (R : Y, Yb, Ce; T : Fe, Ru, Os) type are currently attracting much interest because of a number of exotic properties such as unconventional structural and magnetic ordering in $\text{CeRu}_2\text{Al}_{10}$, metamagnetic transitions, as well as Kondo-insulating behavior in $\text{CeFe}_2\text{Al}_{10}$.³⁸⁻⁴² In $\text{YFe}_2\text{Al}_{10}$, the most recently investigated member of this series, there is mounting evidence that this compound is situated very close to a QCP of FM nature. The proximity to FM ordering is conveyed especially through an Arrott plot presentation of magnetization,^{43,44} but $\text{YFe}_2\text{Al}_{10}$ presents no unambiguous evidence of magnetic order above 50 mK.

In this Rapid Communication, we present our investigations on magnetic susceptibility, specific heat, ^{27}Al NMR, and NQR data in polycrystalline (PC) and single crystalline

(SC) $\text{YFe}_2\text{Al}_{10}$. We have performed temperature- and magnetic-field-dependent measurements in order to connect local magnetic dynamics through NMR and NQR with bulk thermal entropy and the consequences of FM correlations.^{43,44} Bulk data indicate that $\text{YFe}_2\text{Al}_{10}$ is in the vicinity of a magnetic instability.^{43,44} NMR investigations in the temperature range $1.8 \leq T \leq 300$ K and in the field range $0 \leq \mu_0 H \leq 7.27$ T on the PC sample have been carried out to provide better insights concerning the low energy spin excitations, and to contribute to a deeper understanding of the effect of field on the correlated spin dynamics. Furthermore, we succeeded to perform ^{27}Al NQR measurements, which reflect the intrinsic magnetism of the system.

Details pertaining to the synthesis of PC and SC samples of $\text{YFe}_2\text{Al}_{10}$ are described elsewhere.^{43,44} The careful thermal and microprobe analysis inferred high quality and stoichiometric composition of the system without significant atomic disorder.⁴⁵ We found no evidence for site exchange and only one Fe site is present in the host lattice.⁴⁵ This poses a route towards understanding the QC in this system without the complicating factors of atomic disorder, whether accidental or whether induced, as a consequence of doping when used to suppress FM order that is observed in other putative quantum critical systems. The magnetic susceptibility $\chi(T)$ is measured in different H in the T range $1.8 \leq T \leq 300$ K in PC samples using a Quantum Design (QD) magnetic property measurement system (MPMS) superconducting quantum interference device (SQUID) magnetometer. As shown in Fig. 1(a), the low field $\chi(T)$ increases upon lowering T , but $\chi(T)$ tends to saturate below 5 K in high magnetic fields. Above 50 K, $\chi(T)$ obeys a Curie-Weiss behavior [see Fig. 1(b)] and the effective moment ($\mu_{\text{eff}} = 0.52\mu_B/\text{f.u.}$) is rather small. The low value of the saturation moment ($\mu_s \sim 0.02\mu_B/\text{f.u.}$) leads to $\mu_{\text{eff}}/\mu_s \approx 26$, which classifies $\text{YFe}_2\text{Al}_{10}$ as being a weak itinerant FM in the Rhodes-Wohlfarth plot.^{46,47} The enhancement of ac and dc magnetic susceptibility accompanied by $\chi(T) \sim T^{-0.5}$ divergence below 10 K in weak magnetic fields could be due to exchange enhanced $q = 0$ excitations and suggests the presence of spin correlations and

spin fluctuations of Fe moments, which are suppressed with high magnetic fields. However, this power law in $\chi(T)$ is different from that observed in the SC, which can be associated with some sort of powder averaging in the PC sample.⁴⁴ The magnetization isotherm at 2 K displays $H^{0.45}$ [as shown in the inset in Fig. 1(c)], which implies critical spin fluctuations. M vs H follows a mean field type M^2 vs H/M scaling [Fig. 1(c)], suggesting $T \rightarrow 0$ FM ordering. The nature of the Arrott plot is attributed to the zero-point spin fluctuations of the Fe moment close to QCP, which are suppressed with magnetic field.

Specific heat on the PC sample measured in zero field down to 50 mK, using a dilution refrigerator and in various fields down to 0.35 K in the ^3He option of the QD physical property measurement system (PPMS), is shown in Fig. 4(a). The zero field specific heat coefficient $\gamma = C_p(T)/T$ at low T is enhanced and follows a $T^{-0.35}$ behavior, while the $C_p(T)/T$ in 7 T is suppressed and independent of T at low temperature [see Fig. 4(a)]. The low temperature $C_p(T)/T$ in 7 T is corrected for the nuclear Schottky contributions arising mainly from ^{27}Al .⁴⁸ The power law divergence of γ in zero field indicates a quasi-two-dimensional (2D) ferromagnetic SF of Fe moments at $H = 0$. It is noteworthy that, in $\text{YFe}_2\text{Al}_{10}$, Fe atoms are stacked in 2D planes perpendicular to the b direction of the orthorhombic crystal structure. Further to this point, we also draw attention to the fact that SFs in $\text{YFe}_2\text{Al}_{10}$ reside largely within the ac plane.⁴⁴ The Sommerfeld coefficient γ is enhanced (~ 14.5 mJ/mol Fe K^2) compared to $\gamma \sim 3$ mJ/mol Ru K^2 in the isostructural $\text{YRu}_2\text{Al}_{10}$,⁴⁴ indicating quasiparticle mass enhancement, and suggests that the system is driven from a critical regime to a FL state with field. The value of the Sommerfeld-Wilson ratio $R_w = \pi^2 k_B^2 / \mu_0 \mu_{\text{eff}} (\chi/\gamma)$ (≈ 7 at 2 K) is relatively large, implying the presence of FM correlations. These findings could be ascribed to the effect of SFs in this weak itinerant ferromagnet wherein SFs modulate greatly the thermodynamical observables.²² The low T increase of $C_p(T)/T$ could be associated with the virtual scattering of electrons on the Fermi surface via $q = 0$ excitations and CFs of spins, implying an enhancement of the effective mass of electrons.^{4,9} The exchange enhancement and mass enhancement are attributed to a FM instability in close proximity to a QCP.²² The specific heat in a metal is related to the density of states, which seems to be modified around the QCP, leading to unusual scaling laws in T and H , which is substantiated in NMR and NQR data as discussed below.²²

Shown in Fig. 2 are the field sweep NMR spectra of PC together with SC ($H \perp b$) samples at 80 MHz at 4.2 K. The presence of five inequivalent Al sites yields very complex NMR spectra. Each Al site senses different quadrupole couplings, which makes the powder spectra rather broad. The low frequency spectra broaden inhomogeneously, which originate from the broad distributions of H -independent quadrupole interactions admixed with the H -dependent anisotropic Zeeman interactions. The quadrupole Hamiltonian is given as $H_Q = h\nu_Q/6[(3I_z^2 - I^2) + \eta/2(I_x^2 - I_y^2)]$, where $\eta = (V_{xx} - V_{yy})/V_{zz}$ is the asymmetry parameter, $\nu_Q = 3eQV_{zz}/20h$ is the NQR frequency, and V_{zz} is the principal component of the electric field gradient (EFG) tensor, which arises from the local charge distribution. The system presented here has five Al sites resulting in ten NQR lines since each Al site

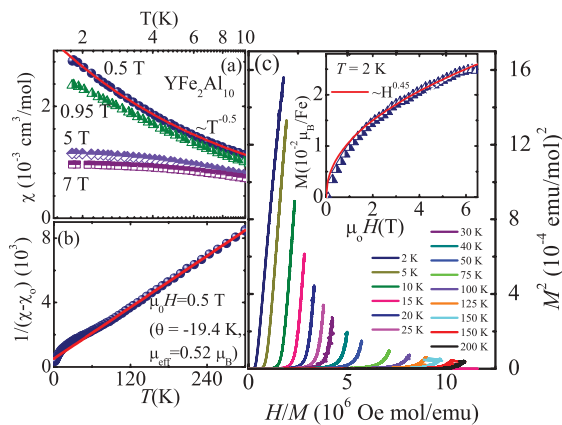


FIG. 1. (Color online) (a) The temperature dependence of $\chi(T)$ in different magnetic fields. The solid line displays the $T^{-0.5}$ behavior. (b) The T dependence of $1/\chi(T)$ with a Curie-Weiss fit. (c) Arrott plot of the magnetization. The inset show M vs H at 2 K with a fit to $H^{0.45}$.

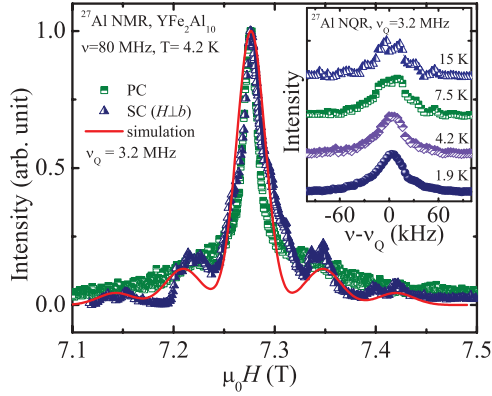


FIG. 2. (Color online) (a) Field sweep NMR PC and SC spectra ($H \perp b$) with a simulation at 80 MHz. The inset shows the NQR spectra ($\pm 3/2 \longleftrightarrow \pm 5/2$) on a PC sample at different T .

has two NQR lines, viz., $\pm 1/2 \longleftrightarrow \pm 3/2$, $\pm 3/2 \longleftrightarrow \pm 5/2$ transitions. The SC NMR spectra exhibit more pronounced (first-order) quadrupolar transitions with lines corresponding to the aforementioned pair of transitions. The central transition is rather broad for a SC, but we interpret this as being due to strong correlations that are prevalent. To simplify the present spectra with five different Al sites (and five different quadrupole coupling constants ν_q) we simulated NMR spectra with the Al site corresponding to a high frequency NMR line. This simulation yields $\nu_q = 1.6$ MHz, which corresponds to the fraction of the Al site having the highest quadrupolar interactions.³⁸ For these Al sites, NQR lines are expected at $\nu_{Q1} = \nu_q$ ($\pm 3/2 \longleftrightarrow \pm 1/2$) and $\nu_{Q2} = 2\nu_q$ ($\pm 5/2 \longleftrightarrow \pm 3/2$). We therefore performed NQR at 3.2 MHz and we indeed observed a relatively narrow NQR line (see the inset in Fig. 2), which is in good agreement with our field sweep NMR results. Above 10 K, the NQR line develops singularities which are symptomatic of multiple quadrupolar transitions. Moreover, the well-resolved NQR lines enable us to probe the low temperature magnetic fluctuations via SLR measurements in $H = 0$. Because of the relatively weak T and H dependence of the linewidth and the absence of a sizable shift of the NMR spectra down to 1.8 K, spin-lattice relaxation time measurements could be performed reliably over a wide T and H range of our investigation, the analysis of which is discussed below. Almost no shift in NMR and NQR spectra could be attributed to the symmetrical position of Fe with respect to Al nuclei and very weak hyperfine fields resulting in the cancellation of transverse hyperfine fields via ^{27}Al . The line broadening at low T is associated with fluctuations of the Fe moments, and consequent strong magnetic correlations, which are in agreement with macroscopic data.^{22,49}

^{27}Al spin-lattice relaxation time measurements have been performed by exciting the central transition (which is not affected by the quadrupole interactions) following a saturation recovery method with suitable radio frequency pulses in different magnetic fields. The recovery of longitudinal magnetization $M(t)$ at a time delay t after the saturation pulse in all T and H ranges could be fitted consistently with a single component valid for $I = 5/2$ nuclei; $1 - M(t)/M(\infty) = 0.0291e^{-t/T_1} + 0.178e^{-6t/T_1} + 0.794e^{-15t/T_1}$, where $M(\infty)$ is the equilibrium magnetization.⁵⁰ The fit of $M(t)$ to the single

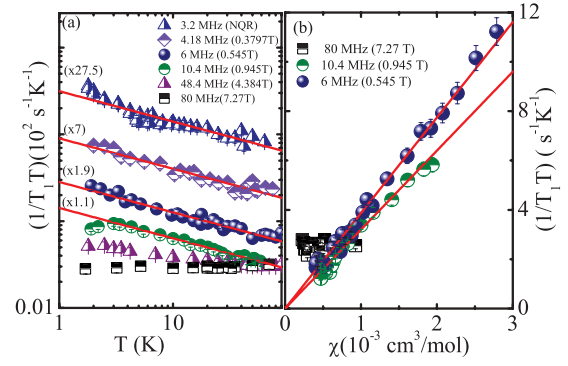


FIG. 3. (Color online) (a) The T dependence of $1/T_1T$ in various magnetic fields. The solid line is a fit to $T^{-0.4}$ ($1/T_1T$ values are shifted for better clarity). (b) The linear relation between $1/T_1T$ and χ with T as an implicit parameter.

component suggests the uniform distribution of Fe moments in the host lattice, and the corresponding SLR results are shown in Fig. 3. $1/T_1$ decreases with decreasing T and shows linear behavior with T in high magnetic fields, which is attributed to the metallic nature of the system due to the effect of noninteracting conduction electrons. This leads to T -independent $1/T_1T$ behavior in high H , and the system is in the FL state. A crossover from Korringa to quantum critical behavior in $1/T_1T$ is observed in a weak magnetic field. As shown in Fig. 3(a), $1/T_1T$ increases monotonically and follows $T^{-0.4}$ behavior below 100 K, evidencing the persistence of CFs of weak itinerant moments in a weak magnetic field.^{15,20} This CF of Fe moments in weak magnetic fields is a consequence of the magnetic instability that is caused by hybridization between nearly filled d -electron shells and conduction electrons. On a first approach, this power law divergence in the spin-lattice relaxation rate suggests a fragile interplay between FM and AFM components of spin fluctuations.¹³

The spin-lattice relaxation rate in principle probes the q -averaged low energy spin excitations, and it can be expressed as the wave-vector q summation of the imaginary part of the dynamic electron spin susceptibility $\chi''(q, \omega_n)$:⁵¹

$$\frac{1}{T_1T} = \frac{2(^{27}\gamma_n)^2}{N_A^2} k_B \sum_q |A_{\text{hf}}(q)|^2 \frac{\chi''(q, \omega_n)}{\omega_n},$$

where $A_{\text{hf}}(q)$ is the hyperfine form factor.

The SLR is linear with $\chi(T)$ in weak magnetic fields [Fig. 3(b)], which is evidence of the dominant role of FM spin fluctuations.^{18,22,52–54} It is worth mentioning that $1/T_1T \sim \chi(T)$ behavior represents the fact that $\chi(T)$ is the uniform spin susceptibility $\chi(q = 0, \omega = 0)$ and accounts for the dominant FM component of the static spin susceptibility.⁵¹ $1/T_1T$ reflects the dynamic SFs which are not related to bulk effects, and the suppression of $1/T_1T$ with field might be attributed to the fact that the relaxation mechanism is governed by the intrinsic magnetism of the system. The FM correlations develop between Fe moments, and the fluctuation of local hyperfine fields of electronic states with respect to ^{27}Al nuclei offers a channel for the relaxation mechanism at the FM wave vector $q = 0$. The modes of SFs are localized in reciprocal space with a small amplitude in $\text{YFe}_2\text{Al}_{10}$, leading to an

unusual power law in SLR, which infers that the system is in the vicinity of a QCP.^{13,22} NMR investigations on the SC are limited due to the poor signal-to-noise ratio in the available tiny SC and skin depth problems. Nonetheless, the values of T_1 in SC are found to be close to those in the PC and infer the absence of strong anisotropy in T_1 for both crystallographic directions $H \perp b$ and $H \parallel b$.

NQR spin-lattice relaxation times are measured for the $\pm 3/2 \leftrightarrow \pm 5/2$ transitions following the saturation recovery method for the $M(t)$. T_1 is determined by fitting the recovery of $M(t)$:^{50,55} $1 - M(t)/M(\infty) = 0.427e^{-3t/T_1} + 0.573e^{-10t/T_1}$. Zero field (NQR) $1/T_1T$ is associated with intrinsic CF, the T dependence of which follows the same power law as in the case of low field $1/T_1T$ data as shown in Fig. 3(a).

As mentioned previously, the quantum criticality in this system could lead to unusual behavior of bulk and NMR data that are connected with magnetic interactions and collective excitations. Interestingly, the observation of the same power law in $1/T_1T$ and $C_p(T)/T$ is not unusual as these two properties are directly related to the electronic density of states at the Fermi energy, and similar features have been observed in related systems.^{10,30,31,56} We rule out the possibility of a Griffith phase in $\text{YFe}_2\text{Al}_{10}$, because of the absence of significant atomic disorder.⁴⁵ It may be noted that the observed CF in χ , $C_p(T)/T$, and $1/T_1T$ are suppressed with field, suggesting the suppression of low lying spin excitations in the SF spectra. A magnetic field of 7 T is strong enough to dampen the fluctuations and diminish the spin entropy towards a FL phase in $\text{YFe}_2\text{Al}_{10}$.^{57–59} The field dependence of the spin-lattice relaxation rate at 2 K follows a dynamic scaling, $1/T_1(H) = 1/T_1(0)[1 + (\mu_B H/k_B T)^2]^{-\xi}$, $\xi = 0.74$ [see Fig. 4(b)]. This scaling behavior is ascribed to the dominant role of the magnetic field in tuning the CFs of spins in inducing the system to a FL phase.^{60–63} Here, the magnetic field accounts for the renormalization of collective excitations and suppresses the correlation effects in $\text{YFe}_2\text{Al}_{10}$, leading to damping of spin fluctuations.^{60–63}

To summarize, the divergences observed in $\chi(T)$ and $C_p(T)/T$ of $\text{YFe}_2\text{Al}_{10}$ are consistently attributed to the quantum CFs of Fe moments and support the conjecture of a $T \rightarrow 0$ phase transition. An absence of magnetic ordering down to 50 mK and low T and H divergences in χ , $C_p(T)/T$, and $1/T_1T$ cannot be interpreted in terms of the standard theory predicted for disordered or

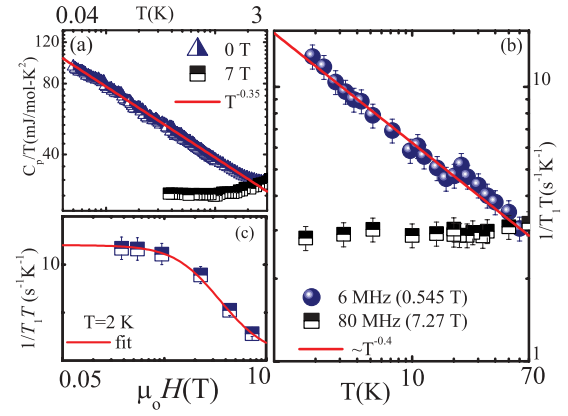


FIG. 4. (Color online) Temperature dependence of C_p/T . The solid line is a fit to $T^{-0.35}$. (b) Field dependence of $1/T_1$ at 2 K with a fit as discussed in the text. (c) $1/T_1T$ vs T at 0.545 and 7.27 T.

NFL models. Bulk and NMR data are consistent with the persistence of FM correlations and infer the dominant role of $q = 0$ components of SF and CF in the spin excitation spectra in tiny magnetic fields. The observed static and dynamic magnetic properties could be associated with a low lying magnetic phase transition, and the system seems to be a d -electron analog of $4f$ -electron heavy fermions. The CFs which are of a FM nature in $\text{YFe}_2\text{Al}_{10}$ are suppressed by applied magnetic field, and a crossover from a QC regime to a FL state is observed, therefore the magnetic field is concluded to play a significant role in driving such a phase transition. Further investigations concerning the effect of chemical pressure and SLR measurements at low temperature are highly desirable. Neutron scattering experiments are required to address the nature of spin fluctuation spectra along various q vectors.

We acknowledge insightful discussions with H. Yasuoka, M. Garst, and M. Brando. We thank C. Klausnitzer for technical support concerning specific heat measurements and U. Burkhard for microprobe and thermal analysis of the sample. We thank the DFG for financial support (OE-511/1-1). Work at Stony Brook University was carried out under NSF Grant No. DMR-0907457. AMS thanks the URC of UJ, and the SA-NRF (78832).

*Corresponding author: pkhuntia@gmail.com

¹G. R. Stewart, *Rev. Mod. Phys.* **73**, 797 (2001).

²G. R. Stewart, *Rev. Mod. Phys.* **78**, 743 (2006).

³H. v. Löhneysen *et al.*, *Rev. Mod. Phys.* **79**, 1015 (2007).

⁴P. Gegenwart *et al.*, *Nat. Phys.* **4**, 186 (2008).

⁵M. Franz, *Nat. Phys.* **3**, 686 (2007), and references therein.

⁶H. Alloul *et al.*, *Rev. Mod. Phys.* **81**, 45 (2009).

⁷J. Dai *et al.*, *Proc. Natl. Acad. Sci. USA* **106**, 4118 (2009).

⁸J. Custers *et al.*, *Nat. Mater.* **11**, 189 (2012).

⁹Q. Si and F. Steglich, *Science* **329**, 1161 (2010).

¹⁰M. B. Maple *et al.*, *J. Low Temp. Phys.* **161**, 4 (2010).

¹¹M. Nicklas, M. Brando, G. Knebel, F. Mayr, W. Trinkl, and A. Loidl, *Phys. Rev. Lett.* **82**, 4268 (1999).

¹²K. Ishida, K. Okamoto, Y. Kawasaki, Y. Kitaoka, O. Trovarelli, C. Geibel, and F. Steglich, *Phys. Rev. Lett.* **89**, 107202 (2002).

¹³T. Misawa *et al.*, *J. Phys. Soc. Jpn.* **78**, 084707 (2009).

¹⁴M. Corti, F. Carbone, M. Filibian, T. Jarlborg, A. A. Nugroho, and P. Carretta, *Phys. Rev. B* **75**, 115111 (2007).

¹⁵K. Yoshimura *et al.*, *J. Phys. Soc. Jpn.* **56**, 1138 (1987).

¹⁶M. Kontani, *J. Phys. Soc. Jpn.* **42**, 83 (1977).

¹⁷B. Chen, H. Ohta, C. Michioka, Y. Itoh, and K. Yoshimura, *Phys. Rev. B* **81**, 134416 (2010).

- ¹⁸K. Yoshimura, T. Imai, T. Kiyama, K. R. Thurber, A. W. Hunt, and K. Kosuge, *Phys. Rev. Lett.* **83**, 4397 (1999).
- ¹⁹T. Hioki *et al.*, *J. Phys. Soc. Jpn.* **43**, 1200 (1977).
- ²⁰H. Sugawara *et al.*, *J. Phys. Soc. Jpn.* **78**, 113705 (2009).
- ²¹M. Majumder, K. Ghoshray, A. Ghoshray, B. Bandyopadhyay, B. Pahari, and S. Banerjee, *Phys. Rev. B* **80**, 212402 (2009).
- ²²T. Moriya, *Spin Fluctuations in Itinerant Electron Magnetism* (Springer, Berlin, 1985).
- ²³A. Yaouanc, P. Dalmas de Reotier, P. C. M. Gubbens, C. T. Kaiser, A. A. Menovsky, M. Mihalik, and S. P. Cottrell, *Phys. Rev. Lett.* **89**, 147001 (2002).
- ²⁴C. Pfleiderer *et al.*, *Nature (London)* **414**, 427 (2001).
- ²⁵M. Uhlarz, C. Pfleiderer, and S. M. Hayden, *Phys. Rev. Lett.* **93**, 256404 (2004).
- ²⁶M. Brando, W. J. Duncan, D. Moroni-Klementowicz, C. Albrecht, D. Gruner, R. Ballou, and F. M. Grosche, *Phys. Rev. Lett.* **101**, 026401 (2008).
- ²⁷D. Moroni-Klementowicz, M. Brando, C. Albrecht, W. J. Duncan, F. M. Grosche, D. Gruner, and G. Kreiner, *Phys. Rev. B* **79**, 224410 (2009).
- ²⁸A. H. Castro Neto, G. Castilla, and B. A. Jones, *Phys. Rev. Lett.* **81**, 3531 (1998).
- ²⁹S. Guo, D. P. Young, R. T. Macaluso, D. A. Browne, N. L. Henderson, J. Y. Chan, L. L. Henry, and J. F. DiTusa, *Phys. Rev. Lett.* **100**, 017209 (2008).
- ³⁰S. Ubaid-Kassis, T. Vojta, and A. Schroeder, *Phys. Rev. Lett.* **104**, 066402 (2010).
- ³¹O. O. Bernal, D. E. MacLaughlin, H. G. Lukefahr, and B. Andraka, *Phys. Rev. Lett.* **75**, 2023 (1995).
- ³²Y. Tabata, T. Taniguchi, Y. Miyako, O. Tegus, A. A. Menovsky, and J. A. Mydosh, *Phys. Rev. B* **70**, 144415 (2004).
- ³³J. Deisenhofer *et al.*, *Phys. Rev. Lett.* **95**, 257202 (2005).
- ³⁴T. Westerkamp, M. Deppe, R. Kuchler, M. Brando, C. Geibel, P. Gegenwart, A. P. Pikul, and F. Steglich, *Phys. Rev. Lett.* **102**, 206404 (2009).
- ³⁵M. B. Salamon, P. Lin, and S. H. Chun, *Phys. Rev. Lett.* **88**, 197203 (2002).
- ³⁶A. H. Castro Neto and B. A. Jones, *Phys. Rev. B* **62**, 14975 (2000).
- ³⁷V. Dobrosavljevic and E. Miranda, *Phys. Rev. Lett.* **94**, 187203 (2005).
- ³⁸M. Matsumura *et al.*, *J. Phys. Soc. Jpn.* **78**, 123713 (2009).
- ³⁹C. S. Lue, S. H. Yang, A. C. Abhyankar, Y. D. Hsu, H. T. Hong, and Y. K. Kuo, *Phys. Rev. B* **82**, 045111 (2010).
- ⁴⁰S. C. Chen and C. S. Lue, *Phys. Rev. B* **81**, 075113 (2010).
- ⁴¹A. Kondo, J. Wang, K. Kindo, Y. Ogane, Y. Kawamura, S. Tanimoto, T. Nishioka, D. Tanaka, H. Tanida, and M. Sera, *Phys. Rev. B* **83**, 180415(R) (2011).
- ⁴²D. D. Khalyavin *et al.*, *Phys. Rev. B* **82**, 100405(R) (2010).
- ⁴³A. M. Strydom *et al.*, *Phys. Status Solidi* **4**, 356 (2010).
- ⁴⁴K. Park, L. S. Wu, Y. Janssen, M. S. Kim, C. Marques, and M. C. Aronson, *Phys. Rev. B* **84**, 094425 (2011).
- ⁴⁵A. Kerkau *et al.*, *Z. Kristallogr.—New Cryst. Struct.* **227**, 289 (2012).
- ⁴⁶P. R. Rhodes *et al.*, *Proc. R. Soc. London, Ser. A* **273**, 247 (1963).
- ⁴⁷Y. Takahashi, *J. Phys. Soc. Jpn.* **55**, 3553 (1986).
- ⁴⁸E. S. R. Gopal, *Specific Heat at Low Temperatures* (Plenum, New York, 1966).
- ⁴⁹T. Umemura *et al.*, *J. Phys. Soc. Jpn.* **52**, 1439 (1983).
- ⁵⁰A. Narath, *Phys. Rev.* **162**, 320 (1967).
- ⁵¹T. Moriya, *J. Phys. Soc. Jpn.* **18**, 516 (1963).
- ⁵²K. Yoshimura *et al.*, *J. Phys. Soc. Jpn.* **53**, 503 (1984).
- ⁵³K. Yoshimura, M. Mekata, M. Takigawa, Y. Takahashi, and H. Yasuoka, *Phys. Rev. B* **37**, 3593 (1988).
- ⁵⁴Y. Takahashi *et al.*, *J. Phys. Condens. Matter* **13**, 6323 (2001).
- ⁵⁵D. E. MacLaughlin *et al.*, *Phys. Rev. B* **4**, 60 (1971).
- ⁵⁶M. C. Aronson, R. Osborn, R. A. Robinson, J. W. Lynn, R. Chau, C. L. Seaman, and M. B. Maple, *Phys. Rev. Lett.* **75**, 725 (1995).
- ⁵⁷G. R. Stewart, J. L. Smith, and B. L. Brandt, *Phys. Rev. B* **26**, 3783 (1982).
- ⁵⁸H. Alloul and L. Mihaly, *Phys. Rev. Lett.* **48**, 1420 (1982).
- ⁵⁹K. Ikeda *et al.*, *J. Magn. Magn. Mater.* **100**, 292 (1991).
- ⁶⁰A. Schröder *et al.*, *Nature (London)* **407**, 351 (2000).
- ⁶¹P. Carretta, R. Pasero, M. Giovannini, and C. Baines, *Phys. Rev. B* **79**, 020401(R) (2009).
- ⁶²V. R. Shaginyan *et al.*, *Eur. Phys. Lett.* **97**, 56001 (2012).
- ⁶³C. Stock, C. Broholm, F. Demmel, J. Van Duijn, J. W. Taylor, H. J. Kang, R. Hu, and C. Petrovic, *Phys. Rev. Lett.* **109**, 127201 (2012).